

# 5G multi-numerology applications in power distribution systems

Vajiheh Farhadi<sup>1</sup> [vf008@bucknell.edu], Thomas La Porta<sup>2</sup> [tfl12@psu.edu], Ting He<sup>3</sup> [tzh58@psu.edu]

<sup>1</sup>Bucknell University, <sup>2,3</sup>Pennsylvania State University

**Abstract**—In recent years, there has been a growing trend in power consumers’ adoption of renewable energy sources such as wind and solar. The energy industry is currently undergoing a phase of innovation to integrate these sources into smart grids. However, the deployment of control networks poses a significant challenge in achieving effective monitoring, control, and data exchange functionalities. The emergence of fifth-generation (5G) networks provides a cost-effective opportunity to enhance capabilities in this regard. By leveraging multi-numerology techniques within the 5G framework, it becomes possible to efficiently share communication infrastructure with other services. This approach offers numerous advantages, including enhanced flexibility, quality of service differentiation, interference mitigation, scalability, and compatibility with existing communication systems.

This paper focuses on the utilization of multi-numerology techniques to optimize resource allocation and improve the overall efficiency of smart grid operations. We consider Mobile Virtual Network Operators as power companies while the nodes represent sensors and actuators deployed in the power grid. To address the challenge of resource allocation, we propose a novel scheme that utilizes multi-numerology Radio Access Network (RAN) network slicing. This scheme aims to maximize observability and controllability within power distribution systems. We approach the problem by characterizing its fundamental complexity and developing suitable heuristics.

Through extensive simulations conducted on the IEEE test feeders, we demonstrate the superior performance of our proposed algorithms in effectively balancing initially unbalanced power distribution systems. These findings highlight the significant benefits of employing multi-numerology techniques in optimizing resource allocation and enhancing the overall efficiency of smart grid operations such as demand management and load balancing.

**Index Terms**—5G, network slicing, multi numerology, SCADA system, power distribution system

## I. INTRODUCTION

The smart grid is a modernized electrical grid equipped with communication and IT systems that enable the monitoring of power flows from generation to consumption points, as well as the automation of power flow control and load curtailment to match power generation in real-time or near real-time. These communication, monitoring, and supervision systems are essential for managing power flows from diverse sources in the smart grid. Furthermore, as renewable and variable power sources are integrated into the electrical grid, the control for the smart grid is becoming more critical. To fully realize the potential of the smart grid, control networks must span the

entire power system, including power generation, transmission, transformation, distribution, and consumption. According to [1], 95% of blackouts occur within the last 5 kilometers of the power grid, specifically in the distribution and consumption part. This particular area presents a significant challenge in the development of smart grid technology. Therefore, this work focuses on developing a control network for power distribution and consumption, which is crucial for optimizing the efficient use of renewable energy sources, ensuring that the grid operates within safe operating limits and preventing overloading or blackouts.

Building a suitable control network for the smart grid is challenging because of the required wide coverage that reaches all the way to smart meters. Last mile coverage is necessary to prevent blackouts and enable the self-healing capability of the smart grid [2]. Moreover, the communication requirements for the control applications differ widely. Intelligent distributed feeder automation, load control, power system protection, and information management for low-voltage distribution, as well as transmission of signals from utility centers to smart meters, all have different uplink-downlink bandwidth and latency requirements. Additionally, some of these applications require high connection density [3]. On top of that, a major challenge facing current power grids is the expansion of distributed renewable energy sources, such as solar panels and wind turbines, which require dynamic balancing of supply and demand. This imbalance leads to decreased reliability, efficiency, and environmental sustainability of the grid, as well as network disturbances such as over-voltage, harmonics distortion, reverse power flow, or power losses [3]. To address these challenges, 5G technology offers a comprehensive communication toolbox that provides more systematic communication with faster reaction times and greater flexibility, making it an ideal solution for smart grid control systems.

5G networks have several characteristics that are well suited to meet the communication requirements of smart grids on a single physical network. Additionally, integrating access backhaul into the 5G network reduces costs by replacing optical fiber with microwave signals as the communication medium. Furthermore, energy companies can build their own private 5G networks to ensure security, latency, and data delivery reliability based on the specific requirements of their applications. The objective of this work is to utilize 5G multi-numerology technology to establish a cost-effective communication network that enhances control over the power grid. This network also improves the connectivity of power grid components to control networks, such as Supervisory Control and Data Acquisition

(SCADA) systems, resulting in better functionality of the grid.

## II. BACKGROUND AND MOTIVATION

### A. Motivational Example

We use the IEEE 123-Node test feeder, Fig. 1, as an example to demonstrate the importance of a well-designed control network in improving the efficiency of power grids. This test feeder is one of the benchmark systems used to evaluate the performance of various algorithms and methodologies. The feeder consists of 123 buses, including a mix of different types such as load buses, generator buses, and substation buses. In a balanced system, the assumption is that the loads are evenly distributed among the three phases, and the magnitudes and characteristics of the loads in each phase are similar. This balance ensures that the system operates efficiently and avoids issues such as voltage imbalances or overloading of individual phases. 123-Node test feeder is intentionally designed to be unbalanced to reflect the real-world distribution of loads in a distribution system.

In 123-Node test feeder, bus 76 bears loads of 105 kW, 70 kW, and 70 kW in the three phases, while bus 65 has a load of 75 kW solely in one of the phases. However, only 19% of the demand at bus 76 and 47% at bus 65 can be met. Next, we consider implementing a control network which aims to regulate system-wide voltage levels by dispatching control commands to buses in order to adjust and regulate their voltage.

To better show the impact of a control network, we install one distributed generator on bus 62, capable of generating a maximum of 60 KW on each phase. With the implementation of the control network, the percentage of served demand for bus 76 and 65 increases to 75% and 69%, respectively. It is because with the control network in place, the control center is capable of managing different aspects of the power system, including power generation, voltage regulation, and phase shifting across all three phases. This leads to a better balance between the supply and demand of electricity, thereby meeting more demands of power grid customers.

### B. Background

5G networks offer a service known as network slicing, which enables network operators to provide various types of services. It divides the 5G network bandwidth into logically isolated networks called a slice. In the context of a smart grid, each slice will serve as a dedicated control line for its active duration. These defined service categories include Enhanced Mobile Broadband (eMBB), Massive Machine Type Communications (mMTC), and Ultra-Reliable Low Latency Communication (URLLC). Advanced applications, such as Vehicle-to-Everything (V2X), require a combination of all three use case types.

The power grid can use slices to customize their control network. URLLC and mMTC slices, in particular, have important uses in the grid. URLLC slices offer reliable and low-latency communication between different components of the grid, such as actuators and control systems. This allows for real-time monitoring, control, and optimization of the grid, including fault detection and isolation, grid stabilization, and outage management. Moreover, mMTC slices facilitate communication

Table I: parameters of numerologies within a subframe in 5G-NR

$\mu$	subcarrier spacing	slots per subframe	slot duration
0	15KHz	1	1 ms
1	30KHz	2	0.5 ms
2	60KHz	4	0.25 ms
...	...	...	...

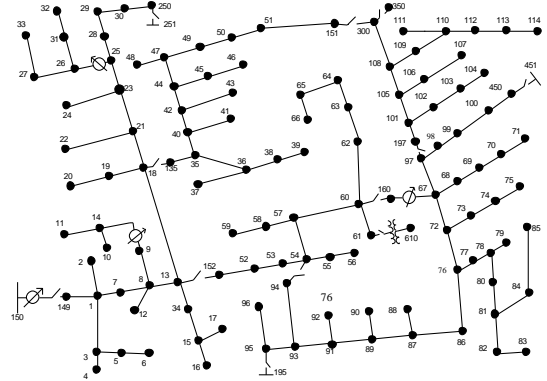


Figure 1: IEEE 123-Node distribution test feeder

between a large number of devices and sensors distributed across the grid, enabling data collection, analysis, and sharing, which can help improve the overall efficiency and sustainability of the grid. Examples of mMTC slice applications include load forecasting, demand response, and energy management. Therefore, the deployment of URLLC and mMTC slices in a smart grid enhances the overall performance of the grid [4], [5].

Radio Access Network (RAN) plays a crucial role in the 5G network architecture, enabling communication between user equipment such as sensors and actuators and remotely controlled machines. The 5G RAN, known as NR (New Radio), uses flexible Orthogonal frequency-division multiplexing (OFDM) technology with subcarrier spacings ranging from 15 kHz to 240 kHz. However, using a single numerology for all scenarios may not be efficient or possible, as narrower subcarrier spacings offer better channel equalization, while wider subcarrier spacings offer a latency advantage. The 5G-NR Release-17 standard defines seven numerology types ( $\mu$ ) that aims to reduce RAN latency, shown in Table I. Each numerology specifies a subcarrier spacing of  $15 \times 2^n$  kHz and a duration of  $1/2^n$  ms for  $n = 0, 1, 2, \dots, 6$ , resulting in a shorter slot duration as the numerology increases.

In our previous work [6], our focus was on developing algorithms for designing a control network using a single numerology. However, in the current work, we enhance our approach by incorporating multiple numerologies to further optimize the utilization of network resources. Furthermore, we extend the impact of the control network to operate at the frame level, as opposed to the subframe level, thereby increasing its effectiveness.

This paper focuses on optimizing the allocation of RAN network bandwidth with different numerologies to various slices, ensuring proper connectivity for the power grid's components where meeting the requirements of various slices. We approach this issue from a layer between the physical layer and the slices, assuming that the infrastructure provider leases its resources to power companies that act as Mobile Virtual Network Operators

(MVNOs). Next, MVNOs offer slices to power grid nodes, such as sensors and actuators. This approach distributes the computational overhead among different MVNOs. As a result, we enhance communication between the control center and power grid nodes, ultimately improving the controllability and observability of the power grid. The control center is responsible for regulating voltage levels throughout the entire power system to ensure the efficient operation of the distribution grid.

### C. Summary of Contributions

Our contributions in this paper include:

1) We consider a SCADA control network for the distribution portion of the power grid and assume that all control links are implemented as network slices. We pose an optimization of maximizing the total served power demand by assigning appropriate slices as a control medium between the control center and nodes in power grid.

2) As the total served power is not an explicit function of the decision variables, we propose a proxy objective function capturing the observability/controllability of nodes in the grid, weighted by their importance in the system topology and their service in the power distribution system. The solution is a set of assigned slices to nodes in the power grid.

3) We formulate the underlying optimization as a non-linear problem, which is proved to be NP-hard.

4) We propose two heuristics, genetic and greedy, to solve the optimization problem. Through extensive evaluations of the IEEE 123-Node and 8500-Node test feeders, we demonstrate that the proposed heuristics outperform baseline approaches. While the genetic heuristic leads to more served load, the greedy runs faster.

**Roadmap:** The remainder of the paper is organized as follows. Section III introduces the coupled power grid and SCADA network. Section IV formulates the optimization problem and analyzes the complexity. Next, it presents the proposed heuristic algorithms. Section V evaluates the performance of the proposed solutions against benchmarks in different test feeders. Section VI reviews related research. Finally, Section VII concludes the paper.

## III. NETWORK MODELS

This paper explores the coupling of a power grid with a geographically co-located SCADA-based control network. The control center has real-time access to information on the power grid's components through network slices. By solving the optimal power flow problem, the control center determines the power injection at all buses within the system and dispatches control commands such as feeder voltage control or automatic switching via slices.

In this section, we present the modeling of the power distribution grid, as well as the associated control network.

### A. Modeling Power Distribution Grid

Power distribution grids are composed of buses and transmission lines connecting the buses together. Source substation buses inject the power in the grid with a fixed voltage.

Fig. 1 shows a power distribution grid, where the source buses are distinguished by circles with arrows. Distribution systems are usually radial. A radial system has only one power source for a group of customers and there is only one path from a distribution substation to a given consumer. Moreover, distribution systems are also multi-phase, where different phases are usually unbalanced. Loads cannot be modeled independently of their voltage. In these systems, a power failure, short-circuit, or a downed power line would interrupt power in the entire line which affects numerous customers.

The optimal power flow is a technique used to regulate the voltage levels across distribution grids to improve their efficiency. It involves managing the generation and consumption of power to optimize objectives such as maximizing served demand, reducing power loss or minimizing the cost of generation [7]. There are various applications of optimal power flow, including Volt/VAR Optimization (VVO), switching optimization, transformer tap optimization, and Conservation Voltage Reduction (CVR) [8]. To solve the optimal power flow problems in our distribution systems, we employ the semidefinite programming models formulated in [9]. As the main focus of this paper is not on the optimal power flow problem, we skip further explanation on it and refer to [9] for more detailed information on the topic.

### B. Modeling Control Network

In the deployment of 5G networks, the prevailing trend is to employ small cell base stations that consist of low-power antennas which are connected to infrastructure such as utility poles or street lights [2]. To address the interference between small cells, this study utilizes the Fractional Frequency Reuse (FFR) technique in conjunction with a homogeneous small cell deployment. FFR partitions the coverage area of each cell into inner and outer zones, enabling every cell to transmit on the same frequency within the inner zone, where the majority of bandwidth resources are allocated. In contrast, different resources are allocated to the outer zones to reduce interference [11], as depicted in Fig. 2. We use terms “small cell” and “cell” interchangeably for ease of reference. Also, our analysis assumes that a constant transmission power of  $P$  is utilized for all gNodeBs within both the inner and outer zones. A gNodeB serves as the functional equivalent of a base station in a traditional cellular network. Furthermore, we assume that all communication nodes such as sensors and actuators are equipped with battery backups and that there are no power limitations imposed on uplink transmission, nor are they affected by power grid failures. In future work, we will explore adaptive power schemes for uplink transmission and gNodeB power

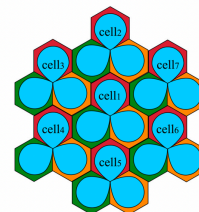


Figure 2: FFR technique: In each small cell, the blue is the part of the bandwidth assigned to the inner zone, while the colored parts are for the outer zones [10].

management. All gNodeBs in small cells are connected to each other through various types of backhaul links, such as fiber optic cables [2]. Additionally, it is assumed that the control center is connected to the gNodeB of the cell located with a fiber optic link; thus, the control center is connected to all gNodeBs.

Based on the requirements of the smart grid discussed in Section II, this research utilizes two types of network slices: mMTC slices for uplink monitoring purposes and URLLC slices for downlink control and regulation of grid equipment. As a result, all nodes in the smart grid necessitate an mMTC slice to transmit their updated data to the control center, while switches, capacitors, and regulators also require URLLC slices. Moreover, the control center is connected to all gNodeBs to utilize mMTC and URLLC slices to receive and send information, respectively.

#### IV. PROBLEM FORMULATION AND ALGORITHMS

This section presents algorithms for designing the control network, i.e. placement of slices as communication links.

##### A. Underlying Optimization Problem

Our objective is to maximize the total served demand in a power distribution grid. This is achieved by optimizing the total supplied power through the solution of the power flow problem by the control center and transmitting control commands via slices. However, the objective function does not directly depend on the placement of slices, which are our decision variables. To address this challenge, we propose the use of a proxy objective function. As in this work we utilize multi-numerology RAN network slicing, a brief discussion on this topic is necessary prior to introducing the proxy objective function.

As mentioned earlier, numerology describes the frequency and subcarrier spacing used in physical layer transmission. The concept of multi-numerology refers to a network's ability to support different numerologies simultaneously, allowing for efficient resource utilization and accommodating various services with different requirements. In our discussion, a "chunk" is the resource configuration of numerology. Fig.3, illustrates a chunk as a rectangular shape located at a specific position in the time-frequency resource grid. Set  $C$  covers all candidate chunks in all possible positions including overlapping chunks. Moreover, a "basic unit" refers to one unit of resource in the time-frequency domain, where set  $U$  denotes all basic units.

Each chunk consists of four basic units. The parameter  $b_{cu} = 1$  indicates that chunk  $c \in C$  includes basic unit  $u \in U$ . For example, there are 40 basic units in Fig.3. Chunk 1 is a  $1 \times 4$  rectangular with numerology 0, while chunk 2 is a  $2 \times 2$  rectangular with numerology 1. The parameter  $b_{cu}$  is fully determined by the chunk's position and the numerical indexing of the basic units. Chunk mappings are obtained in the pre-processing phase with a complexity of  $O(|U||C|)$ .

We formulate an optimization task that selects non-overlapping chunks to create network slices between the nodes and the control center while satisfying the latency requirements of URLLC slices. Here,  $\mathcal{N}$  is set of nodes in power grid and  $S = \{s_U, s_M\}$  is set of sets of URLLC slices and mMTC slices. The principal used notations are explained in Table II.

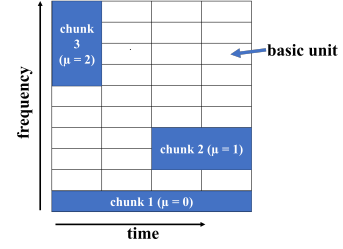


Figure 3: multi-numerology resource grid

$$\max \sum_{n \in \mathcal{N}} \sum_{s \in S} \sum_{c \in C} \gamma_n \gamma'_s y_{ns}^c \quad (1a)$$

$$\text{s.t.} \sum_{n \in \mathcal{N}} \sum_{s \in S} \sum_{c \in C} b_{cu} y_{ns}^c \leq 1 \quad \forall u \in U \quad (1b)$$

$$\sum_{n \in \mathcal{N}} \sum_{s \in S} \sum_{c \in C} 4y_{ns}^c \leq \kappa_m |U| \quad (1c)$$

$$\sum_{n \in \mathcal{N}} \sum_{c \in C} y_{ns}^c P \leq P_{max} \quad s \in s_U \quad (1d)$$

$$y_{ns}^c \leq 0 \quad \forall n \in \mathcal{N}, s \in S, b : b_{cu} = 1 \text{ for } u \notin \theta_n \quad (1e)$$

$$P_r \{D_n^s \geq D_{max}^s\} \leq \epsilon \quad \forall n \in \mathcal{N}, s \in s_U \quad (1f)$$

$$y_{ns}^c + y_{n's'}^{c'} \leq 1 \quad \forall n, n' \in \mathcal{N}, s, s' \in S, \quad (1g)$$

$c, c' \in C$  with different numerology

$$y_{ns}^c + y_{ns}^{c'} \leq 1, \quad \forall n \in \mathcal{N}, s \in S, \quad (1h)$$

$c, c' \in C$  with different numerology

$$y_{ns}^c \leq a_n^s \quad \forall n \in \mathcal{N}, s \in S, c \in C \quad (1i)$$

$$y_{ns}^c \in \{0, 1\}, \quad \forall n \in \mathcal{N}, s \in S, c \in C \quad (1j)$$

Problem (1) represents our optimization problem for each time frame, each cell, and each MVNO. The objective function (1a) aims to maximize the controllability and observability of the power grid by measuring the expected total weight of all the nodes that remain connected to the control center. A higher number of connected nodes allows for better observation and control of the grid, leading to more served power demand. However, priorities among nodes or services differ in reality. For instance, controlling slices between the control center and distributed generators is more critical. Here, the binary variable  $y_{ns}^c = 1$  indicates the assignment of chunk  $c$  to node  $n$  to meet the requirements of slice  $s$ . We assign weights  $\gamma_n$  and  $\gamma'_s$  to specify the importance of node  $n$  and service  $s$ , respectively, and normalize their values in our simulation.

Constraint (1b) ensures that no interference occurs between nodes in small cell while avoiding overlapping of assigned chunks. Constraint (1c) accounts for resource limitations. Here, we assume that the infrastructure provider allocates resource blocks to each MVNO  $m \in M$  based on its service level agreement, which determines the number of assigned resource blocks. The access ratio between the infrastructure provider and MVNO  $m$  is denoted by  $\kappa_m$ , and  $\sum_{m \in M} \kappa_m \leq 1$ . It also ensures that each chunk consists of four basic units.

Constraint (1d) imposes a power constraint on the gNodeB for the duration of one TTI in the downlink direction. Constraint (1e) implements the FFR technique, where  $\theta_n$  denotes the set of basic units associated with the zone in which node  $n$  is located. Constraint (1f) limits the delay

Table II: Table of notations

Notation	meaning
$M$	Set of MVNOs
$S = \{s_U, s_M\}$	Set of sets of URLLC slices and mMTC slices
$\mathcal{N}$	set of nodes in power grid
$U$	set of basic units
$C$	set of candidate chunks
$b_{cu}$	indexing parameter, 1 if chunk $c$ includes basic unit $u$
$r_n^c$	maximum achievable rate on chunk $c$ assigned to node $n$
$y_{ns}^c$	binary variable, 1 if chunk $c$ is assigned to node $n$ in order to satisfy the requirement of slice $s$
$a_n^s$	binary parameter, 1 if node $n$ requests slice $s$
$\theta_n$	set of basic units associated with zone in which node $n$ is located
$\kappa_m$	access ratio between infrastructure provider and MVNO $m$
$P$	Transmission power of gNodeB to a particular node
$P_{max}$	Maximum transmission power of gNodeB for each MVNO
$\gamma'_s$	Priority of slice $s$
$\gamma_n$	Priority of node $n$
$D_s^{max}$	maximum tolerable delay for slice $s$

outage probability of node  $n$  for URLLC service, where  $D_n^s$  and  $D_{max}^s$  denote the delay of node  $n$  and the maximum tolerable delay for URLLC slice  $s$  ( $s \in s_U$ ), respectively.

To minimize Inter Numerology Interference (INI), constraint (1g) optimizes the guardbands between adjacent chunks with different numerologies. This constraint groups the flows of the same numerology in a common band and leaves a fixed guardband between adjacent chunks with different numerologies. Constraint (1h) ensures that only one type of numerology can be used at a time to serve a specific slice  $s$  to node  $n$ . Moreover, constraint (1i) determines the required type of slice for each node. For example, a sensor does not require a URLLC slice. Finally, (1j) determines the binary selection of the decision variable  $y_{ns}^c$ .

*Remark:* The corresponding delay outage probability is given by [12], as shown below.

$$Pr\{D_n^s \geq D_{max}^s\} = e^{-(\sum_{c \in C} y_{ns}^c r_n^c - \lambda_{max}^n) D_{max}^s}, \forall n \in \mathcal{N}, s \in s_U \quad (2)$$

We use the Shannon formula to calculate the maximum achievable rate  $r_n^c$  for chunk  $c$  assigned to node  $n$ . The achievable rate depends on various factors, such as the channel profile, transmission power, noise power, and the configuration of chunk  $c$  which includes the time span, frequency range, and distance of node  $n$  from the gNodeB. Since nodes are stationary in power grids, we predefine a mapping from the configuration parameters to the rate to compute the achieved rate per chunk for each node.

## B. Complexity Analysis

We consider a special case of our general problem (1) and demonstrate that even with the following simplifications, the problem remains NP-hard:

(i) The access ratio between the infrastructure provider and MVNO,  $\kappa_m$ , is fixed at 1, and the number of basic units  $|U|$  is unconstrained, making constraint (1c) unnecessary.

(ii) All nodes require a URLLC slice, and no node requests an mMTC slice, so we have  $S = s_U$ , and  $a_n^{s_U} = 1$ , allowing us to relax constraint (1i).

(iii) We assign all resources to the inner zone by extending the boundary of the inner zone to the cell edge, making equation (1e) redundant as well.

(iv)  $D_{max}^s$  is infinite, so constraint (1f) is no longer needed.

(v) The band gap between chunks with different numerologies is set to zero, allowing us to relax equation (1g).

(vi) Assuming using only one numerology, making constraint (1h) unnecessary.

Therefore, problem (1) simplifies to problem (3).

$$\max \sum_{n \in \mathcal{N}} \sum_{s \in s_U} \sum_{c \in C} \gamma_n \gamma'_s y_{ns}^c \quad (3a)$$

$$\text{s.t.} \sum_{n \in \mathcal{N}} \sum_{s \in s_U} \sum_{c \in C} b_{cu} y_{ns}^c \leq 1 \quad \forall u \in U \quad (3b)$$

$$\sum_{n \in \mathcal{N}} \sum_{c \in C} y_{ns}^c P \leq P_{max} \quad s \in s_U \quad (3c)$$

$$y_{ns}^c \in \{0, 1\} \quad \forall n \in \mathcal{N}, s \in s_U, c \in C \quad (3d)$$

**Theorem 1.** *Problem (3) is NP-hard.*

*Proof.* We prove the NP-hardness of (3) by a reduction from 0-1 knapsack problem: given a set of  $\mathcal{I}$  items, each with value  $\mathcal{V}_i$  and weight  $\mathcal{W}_i$  ( $i = 1, \dots, \mathcal{I}$ ), select subset  $\mathcal{S}$  of items such that  $\sum_{i \in \mathcal{S}} \mathcal{V}_i$  is maximized while  $\mathcal{W}_i \leq \Omega$ , for a given size  $\Omega$  of the knapsack.

*Construction:* For each item  $i$ , construct a chunk  $c$  out of non-overlapping basic units, which is given by a particular MVNO to node  $n$  in order to satisfy the requirement of controlling slice  $s$ . For this item, fix the value and cost equal to  $\gamma_n \gamma'_s$ ,  $\forall s \in s_U$  and  $P$ , respectively. Let  $\Omega = P_{max}$ .

*Claim:* The optimal solution of (3) gives the optimal solution to 0-1 knapsack problem.

*Proof of the claim:* The optimal solution of (3) assigns each chunk to at most one node in order to serve the requirement of the requested slice. Therefore, the assignment decision is to simply assign chunk  $c \in C$  to node  $n \in \mathcal{N}$  to satisfy the requirement of slice  $s \in s_U$  if  $y_{ns}^c = 1$ ; and assign nothing otherwise. Let  $\mathcal{S}$  be the set of indices of all assigned chunks to nodes under the optimal solution to (3). Then, the total value is  $\sum_{i \in \mathcal{S}} \mathcal{V}_i$ , also  $\sum_{i \in \mathcal{S}} \mathcal{W}_i \leq \Omega = P_{max}$ . Selecting all items corresponding to the combination of nodes and chunks assigned by the optimal solution of (3) provides the optimal solution to 0-1 knapsack problem.  $\square$

*Remark:* Proving NP-hardness for the special case shows that the general problem is NP-hard as well.

We now develop efficient algorithms for general problem (1).

### C. Algorithm Design

The NP-hardness of the optimal solution to (1) motivates us to develop efficient heuristics.

1) *Genetic heuristic*: We first apply a heuristic algorithm called the *genetic algorithm* [13]. This algorithm belongs to a non-deterministic class of algorithms that provide suboptimal solutions within a controllable time frame. The genetic algorithm works by modifying a population of possible solutions repeatedly, such that the population evolves towards an optimal solution. At each step, the algorithm randomly selects solutions from the current population to be parents and produces children for the next step.

In our work, a chromosome is defined as a specific allocation of network slices to nodes in the power grid, with each gene corresponding to a node and its value representing the assigned network slice. The initial population is created with random slice assignments. Mutation, which is based on the priorities of nodes ( $\gamma_n$ ) and slices ( $\gamma'_s$ ), involves changing the network slice assigned to a node. The fitness function measures the total served demand achieved through the regulation of injected powers at grid nodes. The goal of the genetic algorithm is to maximize this fitness function, thereby finding the optimal slice assignment.

2) *Greedy heuristic*: We propose a greedy heuristic in Algorithm 1 for the general problem (1). Here set  $|y_{n,s}^c|_k = \{y_{n,s}^{c_1}, \dots, y_{n,s}^{c_k}\}$  indicates the assignment of  $k$  chunks to node  $n$  in order to satisfy the requirements of slice  $s$ . The greedy heuristic approach is designed to make the locally optimal choice at each stage with the aim of finding a global optimum. It works by assigning network slices to nodes in a way that maximizes the served demand at each step. The rationale is that nodes which can serve a higher demand are more critical to the operation of the power distribution system, so assigning network slices to these nodes first will have a greater impact on the total served demand. The greedy heuristic runs polynomial time faster than the genetic heuristic.

---

#### Algorithm 1: Greedy Algorithm

---

- 1 **Input:** Input parameters of (1)
  - 2 **Output:**  $y_{n,s}^c$ 
    - 1: for each node and each slice, calculate  $k$ , the minimum number of required chunks to satisfy the requirement of requested slices
    - 2:  $S \leftarrow \emptyset$ ;
    - 3: **while**  $\exists c \in C \setminus S$  such that  $S \cup |y_{n,s}^c|_k$  satisfies (1b) - (1i) and  $U \setminus S \geq k$  **do**
    - 4:  $S^* \leftarrow \arg \max_{|y_{n,s}^c|_k: S \cup |y_{n,s}^c|_k \text{ satisfies (1b)-(1i)}} \text{objective (1a) under assignment of } (S \cup |y_{n,s}^c|_k)$ ;
    - 5:  $S \leftarrow S \cup S^*$ ;
    - 6: Convert  $S$  to  $y_{n,s}^c$ ;
- 

## V. PERFORMANCE EVALUATION

This section presents the performance evaluation of the proposed algorithms on various power distribution test systems.

### A. Benchmarks and metrics

To evaluate the effectiveness of the proposed algorithms, we compare the performance of following benchmarks:

- 1) *the genetic algorithm*;
- 2) *the greedy algorithm 1*;
- 3) *BC method*, which prioritizes nodes based on their betweenness centrality and allocates basic units to nodes with higher betweenness centrality first to satisfy the requirement of their demanded slices. Mathematically, betweenness centrality of a node is calculated by considering the fraction of shortest paths between all pairs of nodes in the network that pass through that particular node. Here, we model the power grid as a graph, where the nodes and edges of the graph represent the buses and transmission lines in the power grid, respectively.
- 4) *Random method*, which randomly selects nodes and allocates basic units to them until available basic units are exhausted or power constraints are violated. We test the random method with 100 different cases and report the average result.

We evaluate the performance of each solution by measuring the total served power after the control center executes the optimal power flow model and regulates the power injection of nodes in the grid. All algorithms are implemented in MATLAB R-2022b. The power flow model is calculated using CVX, which is integrated into MATLAB.

### B. Simulation Setup

We evaluate the proposed solutions using two well-established test feeders commonly employed in power systems research: the IEEE 123-Node and 8500-Node test feeders [14]. These test feeders represent simplified models of actual distribution circuits and include unbalanced loading, switches, shunt capacitors, and voltage regulators to compensate for severe voltage drops caused by loaded transmission lines. To further simulate real-world scenarios, we also incorporate the installation of various types of distributed generation, such as rooftop solar PV systems within the test feeders. We install 10 distributed generation units at nodes in the IEEE 123-Node test feeder, and 100 distributed generation units in the IEEE 8500-Node test feeder. The topology of the IEEE 123-Node test feeder is shown in Fig. 1. Next, these power distribution systems are mapped to an urban area, where the nodes are assigned to city blocks. We consider a rectangular city block in Chicago measuring 330 by 660 feet [15]. We assume that the antennas are placed on the roofs of the buildings, and only line-of-sight transmission is considered. We use homogeneous cell deployment, where one gNodeB is placed at the center of each cell with a radius of 250 meters. The maximum transmission power of each gNodeB is  $P_{max} = 20$  W, and the transmission power from a gNodeB to any particular node is  $P = 30$  dBm [16]. Each test feeder is covered by multiple cells. We assume the control center is located at the highest-degree node in the test feeders and is connected to all gNodeBs in cells.

We assume a system bandwidth of  $W = 20$  MHz with a carrier frequency of 2 GHz. To implement the FFR technique, we divided the total bandwidth of each cell between the inner zone and three outer zones. We allocated 2/3 of the resources to the inner zone while assigning 1/9 of resources to each

outer zone. The boundary of the inner zone was defined based on the path loss threshold, set to the path loss between the gNodeB and a node located at 2/3 of the cell radius. For simplicity, we assume only one MVNO exists in each cell with an SLA equal to 1. However, the results can be easily extended to numerous MVNOs with different SLAs. In this study, we assumed that all nodes required mMTC slices for monitoring purposes, while URLLC slices were only requested by generators, switches, shunt capacitors, and regulators to receive control commands from the control center. Please note that the number of required basic units for each slice depends on the channel gain between the gNodeB and nodes.

### C. Results

This section compares and analyzes the performance of all benchmark algorithms in relation to each other.

#### 1) Setting Design Parameters:

Table III: design parameters based on the performance of 123-Node test feeder (percentage of total served demand compared to the fully controllable case)

(a) different numerology

scenario	numerology	genetic	greedy	no control
1	$\mu = 0$	57	43	24
2	$\mu = 1$	62	50	24
3	$\mu = 0 \& 1$	75	68	24

(b) different node weights

	degree	BC	power	degree.*power	BC.*power
genetic	56	59	44	66	75
greedy	49	54	40	62	68

(c) different slice weight ratio (importance of URLLC slice over mMTC slice)

	0.5	1	2	3	4	5
genetic	54	59	65	75	76	76
greedy	48	53	60	68	68	69

Table III shows the impact of different design parameters of genetic and greedy heuristics on the assignment of slices for the IEEE 123-Node test feeder. The allocation of different sets of slices results in different control networks. This table showcases the ratio of total served demand achieved through the regulation of injected powers at grid nodes through the designed control network compared to the scenario where the control network has secure and full connectivity between all nodes and the control center. The test feeder is covered by 12 cells, and each cell is assigned 72 basic units. Moreover, the maximum tolerable delay for URLLC slices is set to 0.75 ms.

*Impact of numerology:* Table IIIa demonstrates the effect of different numerologies in slice assignment on the total served demand. In scenario 1, only numerology 0 is utilized for all slices. In scenario 2, only numerology 1 is employed for all slices. In scenario 3, a combination of numerology 1 and numerology 0 is utilized simultaneously, where numerology 1 assigned to URLLC slices and numerology 0 assigned to mMTC slices. The results demonstrate that scenario 3 serves higher demand power due to the increased flexibility in the allocation of basic units. Scenario 2 outperforms scenario 1, primarily due to its shorter subcarrier spacing, which satisfies

the delay requirement with fewer chunks. Additionally, the genetic algorithm provides superior performance compared to the greedy heuristic. Throughout the remainder of this paper, we adopt the usage of two numerologies: numerology 1 for URLLC slices and numerology 0 for mMTC slices.

*Impact of node weight definition:* Table IIIb showcases the impact of different node weight definitions or  $\gamma_n$  in slice assignment on the total served demand. We consider the following definitions: (i) degree, (ii) betweenness centrality (BC), (iii) power injection, (iv) power injection multiplied by degree, and (v) power injection multiplied by BC. The results indicate that the node weight definition of the product of the betweenness centrality and the real power injected at the node yields the best performance. This definition incorporates both the topological importance (betweenness centrality) and the service relevance (power injection) of nodes. Therefore, we use this definition for the remainder of this paper.

*Impact of slice weight definition:* Table IIIc illustrates the impact of different slice weight definitions or  $\gamma'_s$  in slice assignment on the total served demand. While monitoring the status and collecting data from various nodes in the power grid is crucial for proper operation, the controlling aspect plays an even more critical role. SCADA systems facilitate functions such as feeder voltage control and automatic switching through dispatching control commands. Since no existing data provides information on the relative importance of controlling versus monitoring actions in SCADA systems, we compare the performance of our proposed algorithms using different ratios of  $\gamma'_{sU}/\gamma'_{sM}$ , which represents the weight of URLLC slices over mMTC slices. The results demonstrate a significant performance improvement as this ratio increases, indicating the importance of controlling commands. Consequently, we set  $\gamma'_{sU}/\gamma'_{sM} = 3$ .

#### 2) Overall Comparison of all baselines:

*Impact of numbers of basic units:* Fig. 4 presents a comparison of the algorithms' performance in terms of served power for the IEEE 123 and 8500-Node test feeders with different numbers of basic units for each cell. This figure clearly illustrates that the utilization of more basic units leads to higher delivered power. This can be attributed to the increased number of nodes that can be monitored and controlled, resulting in an overall improvement in the total served power. Moreover, the genetic heuristic consistently outperforms all other baselines, emphasizing the significance of strategic slice placement. Following closely, the greedy algorithm demonstrates good performance as the second-best algorithm. The BC method, which prioritizes nodes with higher betweenness centrality, ranks third among the algorithms. Intuitively, these nodes have a significant impact on other nodes in radial power distribution grids. As expected, the random benchmark provides the lowest performance, confirming the importance of employing sophisticated algorithms. This trend holds true for both test feeders.

*Impact of URLLC delay tolerance:* Fig. 5 compares the performance of all algorithms by varying the maximum tolerable delay of URLLC slices for 123- and 8500-Node test feeders. Each cell is assigned 72 basic units. Results show that as the delay increases, the control network delivers more power. This is because fewer chunks are needed to create slices, resulting in a higher number of observable

and controllable nodes. Furthermore, the genetic heuristic consistently outperforms the other baseline algorithms.

Finally, Fig. 6 presents the utilization of basic units by different methods. We examine the distribution of basic units for one of the cells in 123-Node test feeder. In this analysis, the maximum acceptable delay for URLLC connections is set to 0.75 ms, and the total number of resource units available in each cell is 72. The results indicate that the genetic algorithm and the greedy algorithm exhibit the most efficient utilization of resources, whereas the random method inefficiently allocates a substantial portion of resources to guardbands.

3) *Comparison over frame*: In the previous subsections, we presented the results for when the frame is composed of a single subframe. In Fig. 7, we extend our analysis to a frame consisting of multiple subframes. We increase the frame length from 1 to 10 subframes while considering two different numerologies: numerology 0 for mMTC slice and numerology 1 for URLLC slice. The tolerable delay for URLLC slice remains at 0.75 ms, and each cell is allocated a total of 72 resource units. This figure illustrates the ratio of total served demand after regulating the power of the grid's components. A comparison is made with the scenario of secure and full connectivity between all nodes and the control center. It is assumed that the control center has complete knowledge of the grid prior to the initiation of the frame, and at each subframe, it receives updated information from the sensors connected through mMTC. The results depicted in Fig. 7 demonstrate that a longer frame duration allows for enhanced control over the grid, leading to improved performance.

## VI. RELATED WORK

Network slicing offers numerous benefits, but efficiently allocating resources for multiple network slices over a shared physical infrastructure remains a challenging problem. The main objective of resource allocation in network slicing is to allocate virtual resources, such as computing and bandwidth, for each network slice and user based on their service requirements and the network's status [17]. Several studies have proposed solutions to address this problem, including a novel RAN network slicing architecture for a flexible and cost-effective multi-service mobile network [18], resource allocation for high-quality selection of radio points of access, Virtual Network Function placement, and data routing [19], and optimal resource allocation in C-RAN with the goal of reducing overall cost [20]. Prioritized admission mechanisms have also been proposed to improve resource utilization and user experience in RAN [21]. Additionally, some studies have explored network slicing for dynamic resource demand and availability in a mobile environment [22]. The authors

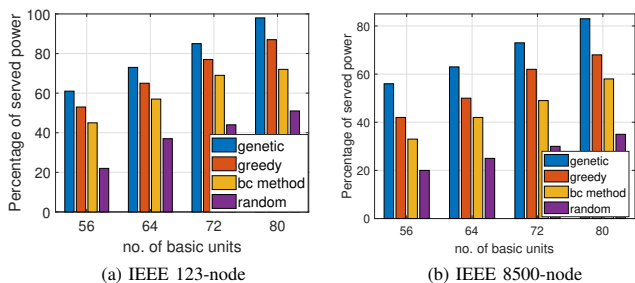


Figure 4: Performance evaluation for test feeders under different numbers of basic units

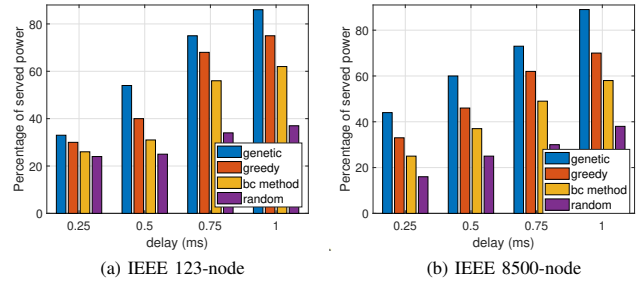


Figure 5: Performance evaluation for different test feeders under various delays

in [23], [24] focus on RAN network slicing architecture that utilizes spectrum resources in both licensed and unlicensed bands.

5G-NR has been designed to support various verticals with diverse requirements. Despite the different numerologies defined in 5G-NR, a significant amount of literature uses a single numerology throughout the network slice's lifetime [6], [11], [12], [25], [26]. In contrast, the authors in [27] utilize multi-numerology network slicing and develop a mathematical framework to analyze the blocking probabilities of both eMBB and URLLC services. To address the diverse requirements of UEs, novel scheduling solutions based on Deep Reinforcement Learning have been introduced by [28]–[31] for resource allocation and numerology selection. In addition, [32] proposes a channel quality and Quality of Service (QoS)-aware resource allocation scheme for a multi-numerology 5G network.

There is a significant amount of research being conducted on optimizing energy trading in microgrid systems. The authors in [33], [34] use various machine learning techniques to address various challenges such as reducing energy costs, ensuring a stable energy supply, integrating renewable energy sources, and managing energy storage devices effectively.

## VII. CONCLUSION & FUTURE WORK

The integration of 5G into the control network of smart grids brings numerous benefits, allowing power companies to allocate resources to different network slices and leverage latency, connectivity, speed, and throughput requirements. This not only enhances the controllability and connectivity of grid components but also offers cost savings through network slicing.

This research focuses on the allocation of bandwidth in 5G-NR RAN network slicing to optimize the controllability and connectivity of grid components. We not only prove the NP-hardness of the proposed solution but also develop efficient heuristics to tackle the problem. Extensive simulations on the IEEE 123- and 8500-Node test feeders demonstrate the effectiveness of the proposed algorithms in achieving a balanced power grid with maximized power delivery.

Despite the considerable potential benefits, there are still several challenges that require attention. In future work, we

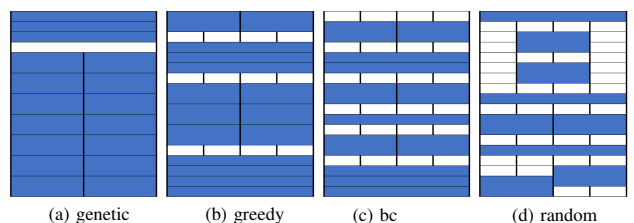


Figure 6: Basic units assignment under different methods for IEEE 123-Node test feeder



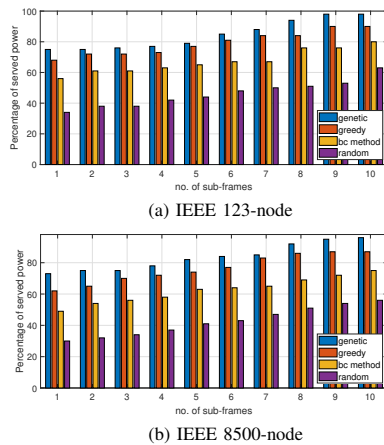


Figure 7: Performance evaluation of different test feeders under varying frame durations will emphasize the maintenance of Service Level Agreements (SLAs), Quality of Service (QoS), and security assurance for each network slice. Additionally, we will explore spectrum slicing and allocation strategies for scenarios involving user consumption prediction, ensuring efficient resource utilization.

## REFERENCES

- [1] C. T. SGCC and Huawei, "Powered by sa: Smart grid 5g network slicing," 3 2020.
- [2] X. xia, L. Zhang, C. Mei, J. Li, x. Zhu, Y. Liang, and J. Song, "A survey on 5g network slicing enabling the smart grid," 12 2019, pp. 911–916.
- [3] P.-J. Alet, F. Baccaro, M. De Felice, V. Efthymiou, C. Mayr, G. Graditi, M. Juel, D. Moser, M. Petitta, S. Tselepis, and G. Yang, "Quantification, challenges and outlook of pv integration in the power system: a review by the european pv technology platform," in *Proceedings of EU PVSEC, 2015*, eU PVSEC 2015 ; Conference date: 14-09-2015 Through 18-09-2015.
- [4] J. Yeo, T. Kim, J. Oh, S. Park, Y. Kim, and J. Lee, "Advanced data transmission framework for 5g wireless communications in the 3gpp new radio standard," *IEEE Communications Standards Magazine*, vol. 3, no. 3, pp. 38–43, 2019.
- [5] H. C. Leligou, T. Zahariadis, L. Sarakis, E. Tsampasis, A. Voulkidis, and T. E. Velivassaki, "Smart grid: a demanding use case for 5g technologies," in *2018 IEEE International Conference on Pervasive Computing and Communications Workshops (PerCom Workshops)*, 2018, pp. 215–220.
- [6] V. Farhadi, T. La Porta, T. He, and N. R. Chaudhuri, "Resource allocation in 5g multi-tenancy network slicing for balancing distribution power systems," in *2022 IEEE 19th International Conference on Mobile Ad Hoc and Smart Systems (MASS)*. IEEE, 2022, pp. 162–170.
- [7] R. R. Jha, A. Dubey, C.-C. Liu, and K. P. Schneider, "Bi-level volt-var optimization to coordinate smart inverters with voltage control devices," *IEEE Transactions on Power Systems*, vol. 34, no. 3, pp. 1801–1813, 2019.
- [8] E. P. S. A. . O. Software, "System optimization," <https://etap.com/packages/system-optimization>.
- [9] Z. Wang, D. S. Kirschen, and B. Zhang, "Accurate semidefinite programming models for optimal power flow in distribution systems," 2017.
- [10] N. Al-Falahy and O. Y. K. Alani, "Network capacity optimisation in millimetre wave band using fractional frequency reuse," *IEEE Access*, vol. 6, pp. 10924–10932, 2018.
- [11] A. A. Gebremariam, T. Bao, D. Siracusa, T. Rasheed, F. Granelli, and L. Goratti, "Dynamic strict fractional frequency reuse for software-defined 5g networks," in *2016 IEEE International Conference on Communications (ICC)*, 2016, pp. 1–6.
- [12] T. Ma, Y. Zhang, F. Wang, D. Wang, and D. Guo, "Slicing resource allocation for embb and urllc in 5g ran," *Wireless Communications and Mobile Computing*, vol. 2020, pp. 1–11, 01 2020.
- [13] D. Whitley, "A genetic algorithm tutorial," *Statistics and Computing*, vol. 4, pp. 65–85, 1994.
- [14] K. P. Schneider, B. A. Mather, B. C. Pal, C.-W. Ten, G. J. Shirek, H. Zhu, J. C. Fuller, J. L. R. Pereira, L. F. Ochoa, L. R. de Araujo, R. C. Dugan, S. Matthias, S. Paudyal, T. E. McDermott, and W. Kersting, "Analytic considerations and design basis for the ieee distribution test feeders," *IEEE Transactions on Power Systems*, vol. 33, no. 3, pp. 3181–3188, 2018.
- [15] C. D. of Transportation, "Street and site plan design standards," April 2007. [Online]. Available: <https://www.chicago.gov/dam/city/depts/cdot/StreetandSitePlanDesignStandards407.pdf>
- [16] S. O. Oladejo and O. E. Falowo, "5g network slicing: A multi-tenancy scenario," in *2017 Global Wireless Summit (GWS)*, 2017, pp. 88–92.
- [17] P. Popovski, K. F. Trillingsgaard, O. Simeone, and G. Durisi, "5g wireless network slicing for embb, urllc, and mmcc: A communication-theoretic view," *Ieee Access*, vol. 6, pp. 55765–55779, 2018.
- [18] X. Foukas, M. K. Marina, and K. Kontovasilis, "Orion: Ran slicing for a flexible and cost-effective multi-service mobile network architecture," in *Proceedings of the 23rd annual international conference on mobile computing and networking*, 2017, pp. 127–140.
- [19] J. Martín-Pérez, F. Malandrino, C.-F. Chiasserini, and C. J. Bernardos, "Okpi: All-kpi network slicing through efficient resource allocation," in *IEEE INFOCOM 2020-IEEE Conference on Computer Communications*. IEEE, 2020, pp. 804–813.
- [20] A. A. Ari, A. Gueroui, C. Titouna, O. Thiare, and Z. Aliouat, "Resource allocation scheme for 5g c-ran: a swarm intelligence based approach," *Computer Networks*, vol. 165, p. 106957, 2019. [Online]. Available: <https://www.sciencedirect.com/science/article/pii/S1389128619310072>
- [21] M. Jiang, M. Condoluci, and T. Mahmoodi, "Network slicing management prioritization in 5g mobile systems," in *European Wireless 2016; 22th European Wireless Conference*, 2016, pp. 1–6.
- [22] H. Zhang, N. Liu, X. Chu, K. Long, A.-H. Aghvami, and V. C. M. Leung, "Network slicing based 5g and future mobile networks: Mobility, resource management, and challenges," *IEEE Communications Magazine*, vol. 55, no. 8, pp. 138–145, 2017.
- [23] Y. Xiao, M. Hirzallah, and M. Krunz, "Distributed resource allocation for network slicing over licensed and unlicensed bands," *IEEE Journal on Selected Areas in Communications*, vol. 36, no. 10, pp. 2260–2274, 2018.
- [24] E. Ataebojrd, M. Rasti, H. Pedram, and P. H. J. Nardelli, "Stochastic geometry analysis of spectrum sharing among seller and buyer mobile operators," in *2022 IEEE Wireless Communications and Networking Conference (WCNC)*, 2022, pp. 2011–2016.
- [25] K. Boutiba, A. Ksentini, B. Brik, Y. Challal, and A. Balla, "Nrflex: Enforcing network slicing in 5g new radio," *Computer Communications*, vol. 181, 10 2021.
- [26] S. O. Oladejo and O. E. Falowo, "Latency-aware dynamic resource allocation scheme for multi-tier 5g network: A network slicing-multitenancy scenario," *IEEE Access*, vol. 8, pp. 74834–74852, 2020.
- [27] V. N. Ha, T. T. Nguyen, L. B. Le, and J.-F. Frigon, "Admission control and network slicing for multi-numerology 5g wireless networks," *IEEE Networking Letters*, vol. 2, no. 1, pp. 5–9, 2020.
- [28] K. Boutiba, M. Bagaa, and A. Ksentini, "Radio resource management in multi-numerology 5g new radio featuring network slicing," in *ICC 2022 - IEEE International Conference on Communications*, 2022, pp. 359–364.
- [29] T. Dong, Z. Zhuang, Q. Qi, J. Wang, H. Sun, F. R. Yu, T. Sun, C. Zhou, and J. Liao, "Intelligent joint network slicing and routing via gen-powered multi-task deep reinforcement learning," *IEEE Transactions on Cognitive Communications and Networking*, vol. 8, no. 2, pp. 1269–1286, 2022.
- [30] T. Mai, H. Yao, N. Zhang, W. He, D. Guo, and M. Guizani, "Transfer reinforcement learning aided distributed network slicing optimization in industrial iot," *IEEE Transactions on Industrial Informatics*, vol. 18, no. 6, pp. 4308–4316, 2022.
- [31] H. H. Esmat and B. Lorenzo, "Deep reinforcement learning based dynamic edge/fog network slicing," in *GLOBECOM 2020 - 2020 IEEE Global Communications Conference*, 2020, pp. 1–6.
- [32] A. Akhtar and H. Arslan, "Downlink resource allocation and packet scheduling in multi-numerology wireless systems," in *2018 IEEE Wireless Communications and Networking Conference Workshops (WCNCW)*, 2018, pp. 362–367.
- [33] X. Lu, X. Xiao, L. Xiao, C. Dai, M. Peng, and H. V. Poor, "Reinforcement learning-based microgrid energy trading with a reduced power plant schedule," *IEEE Internet of Things Journal*, vol. 6, no. 6, pp. 10728–10737, 2019.
- [34] M. Al-Saadi, M. Al-Greer, and M. Short, "Reinforcement learning-based intelligent control strategies for optimal power management in advanced power distribution systems: A survey," *Energies*, vol. 16, no. 4, 2023. [Online]. Available: <https://www.mdpi.com/1996-1073/16/4/1608>